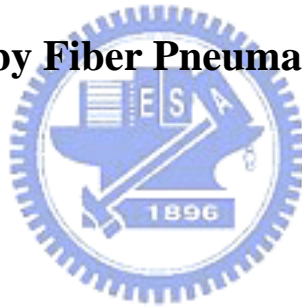


CHAPTER 4

A Study on the Mechanism of Electroless Nickel Coating in a Carbon Fiber Tow by Fiber Pneumatic Spreading System



A Study on the Mechanism of Electroless Nickel Coating in a Carbon Fiber Tow by Fiber Pneumatic Spreading System

Abstract

A carbon fiber tow was successfully separated by the pneumatic spreading system. Spreading evenness, a new variable, was defined to determine the spreading degree of a carbon fiber tow in the fiber pneumatic spreading process. By the spreading evenness, a quantitative comparison of the spread carbon fiber tow can be made and the optimum condition can be easily determined at the pneumatic spreading process. It was found that a slight difference in spreading evenness was 36.3 (%) and 37.8 (%) under the condition $Q = 70$ L/min and $Q = 90$ L/min, respectively, at the same fiber transporting velocity $V_F = 7$ m/min. The spreading evenness could get up to 72 (%) under $V_F = 7$ m/min and $Q = 105$ L/min while the air velocity was properly adjusted by changing the number of slots in the pneumatic spreader. To identify the non-uniform coating in a carbon fiber tow can be overcome by the pneumatic spreading process, two groups of spread and unspread carbon fiber tow coated with nickel by electroless plating were compared. The results showed that a uniform Ni coating could be obtained on each fiber in the spread carbon fiber tow, and the thickness of the Ni film could be coated on carbon fiber tow less than $0.2 \mu\text{m}$. Meanwhile, a different reaction mechanism was found in the electroless plating process. Two different controlled reaction mechanisms simultaneously occurred in an unspread carbon fiber tow as the electroless plating reaction proceeding, which resulted in non-uniform nickel coating, one is diffusion-controlled reaction; the other

is activation-controlled reaction.



. Introduction

In recent years, a great deal of interest has been given to the nickel coated carbon fibers used as functional and reinforced materials in plastic, glass and metal matrix composites [1-4]; however, the chemical reactions and wettability between the carbon fiber and the matrix have limited their applications. Therefore, many methods have been proposed for the preparation of metallic or non-metallic coated fiber tow to prevent the chemical reaction [5-9]. Certain coatings can promote the wettability as well as prevent the matrix coming into direct contact with carbon. Although electroless nickel (EN) plating seems to be an attractive method for the coating on carbon fiber, the variation in the coating thickness was observed in a carbon fiber tow [6,10,11]. The results were found that the fiber and composite strength decreased with increasing coating thickness [12-14]. The non-uniform coating in thickness is caused by the compact carbon fibers in a tow. Abraham et al. has shown that the Ni coating thickness was ranged between 0.2 and 0.6 μm for the electroless plating method in a carbon fiber tow containing 6,000 fibers [6,7]. Similar results were found by Shi et al. for the thickness ranged between 0.2 μm and 1 μm [4]. A very thin coating over the fiber surface will be ideal, but it may not be possible to get an identical nickel film and coat less than 0.2 μm thin layer on each fiber in a carbon fiber tow [4,6,15-16]. Thus, if the carbon fibers are separated uniformly, it is advantageous for the improvement of fiber coatings.

To obtain a thin and uniform coating in a carbon fiber tow, pneumatic spreading system was developed for pneumatically spreading carbon filaments from a tow bundle to form a sheet or a ribbon in which the filaments were maintained in parallel [17]. The carbon fiber tow is comprised of thousands of filaments and the filaments

are interacted with air in the spreader. Spreading characteristics of the carbon fiber tow in the spreader at different service conditions were qualitatively investigated. The results were found that the fiber tow is easily spread out, and the performance is better than the prior studies. Furthermore, the spreading procedures can help in understanding the spreading process. Spreading degree of a carbon fiber tow can be improved, but the evenness of the spread carbon fiber tow is the primarily interested. However, the evenness of the spread fiber tow had never been considered. To quantitatively evaluate the distribution of the spread fiber tow, a measurable method will be constructed in this study. Meanwhile, EN coating will be utilized for discussing the effect between a spread carbon fiber tow and an original carbon fiber tow.

EN plating is a chemical reduction process, and the electroless process proceeds only on certain catalytic metals. Therefore, substrates have to be activated to initiate the nickel nucleation process. Marton and Schlesinger have shown that the critical film thickness at which the EN deposit is continuous depends on the nature of the active substrate [18]. In other words, the substrates greatly affect the catalyst contents adsorbed. For the EN deposition, there are various reaction mechanisms that have been extensively studied. Four principal reaction mechanisms have been proposed to account for the reduction with different reductants in both alkaline and acid media [19]. They are pure electrochemical mechanism, metal hydroxide mechanism, hydride ion mechanism and atomic hydrogen mechanism, respectively.

The proposed mechanisms explain the anodic behavior of reductants on different electrode surfaces, and the influence of pH and potential. However, none of previous works investigated the detail mechanisms of EN plating in a carbon fiber tow. The objective of the present study is primarily concerned with the nucleation and growth

of EN deposit in a spread and unspread carbon fiber tow, and we will investigate the controlled mechanism that causes the non-uniform Ni coating by the spread carbon fiber tow. Finally, a method will be provided to obtain the thin and uniform Ni coating on a carbon fiber tow.



. Experiment

A. Experimental Setup

Experiments were conducted using the setup shown schematically in Fig. 4-1. The main elements were comprised in sequence of: the tow feed spool, tension control device, the pneumatic tow spreader, vacuum pump and take-up spool. The fibers from the carbon fiber tow containing 12,000 filaments were passed through a fiber guide into a first friction roller. The first roller was synchronized with second friction roller at a constant rate of speed. Two rollers were controlled by a variable speed driver. Hence, the fibers between the two rollers, which were subsequently spread in the pneumatic spreader, remained in a low tensional state that was given by tension control device. For the air flow rate in the pneumatic spreader, the vacuum pump sucked air, and gave a stable control of flow rate which was measured by a multiple tube flow meter and precision pressure controller. After the fibers spread and left the second roller, the fibers were taken up by a take-up system.

The pneumatic spreader designed by three-dimensional flow-field numerical simulation can provide a stable flow field and was shown in previous study [17], and half geometry of the pneumatic spreader was shown in Fig. 4-2. The design of the spreader must satisfy several interacting requirements. Inlet-2 was the fiber tow entrance and inlet-1 was the tow exit. The air was sucked into the spreader and the airflow entered the inlet-1 and passed through the nine slots on the clapboard to the outlet. The spreader was formed by PAN (polyacrylonitrile) pieces, which were transparent allowing the spread procedure of carbon fibers to be photographed, and was fixed by two steel plates to avoid vibration during fiber spreading process.

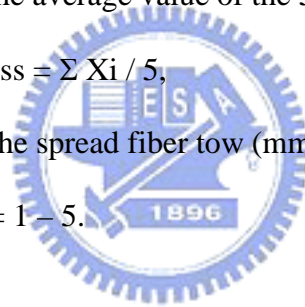
B. Image Process

Spreading degree of the fiber tow can be gotten better by our previous study, but the evenness of the spread fiber tow is more important than the spreading degree. If the fiber tow was not be uniformly spread out, the fibers would be partially piled up closely. Therefore, the spreading evenness of a carbon fiber tow should be first considered in the spreading process. A carbon fiber tow would be separated in 50 mm wide. To evaluate the evenness of the spread fiber tow, the LECO 2001 Image Processing System was used. Firstly, the image (50 mm × 50 mm, width × length) of the spread fiber tow was captured by CCD, and an image was taken each 50 mm interval in length. Consecutively for 5 images, area fraction for each image of the fiber tow was calculated by image processing system at setting gray level. The spread evenness was determined by the average value of the 5 area fractions.

$$\text{Spreading evenness} = \sum X_i / 5,$$

$$X_i(\%) = \text{Area of the spread fiber tow (mm}^2\text{)} / 50 \times 50 \text{ (mm}^2\text{)},$$

$$\text{where } i = 1 - 5.$$



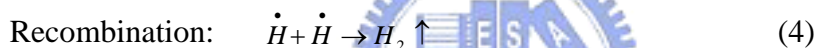
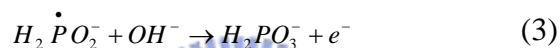
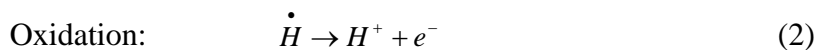
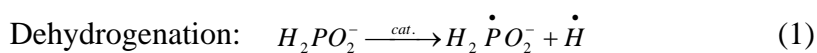
C. Electroless Nickel Plating

A carbon fiber tow used in this study was T300C with the average diameter of 7 μm make by Japan Toray Co. Ltd. It was divided into groups of unspread and spread carbon fiber tow. The spread fiber tow was separated in 50mm wide by pneumatic spreading system, and has good spreading evenness. In order to initiate the electroless nickel deposition, both unspread and spread carbon fiber tows were catalyzed through a two-step pretreatment consisting of 60sec of sensitization and followed by 60sec of activation steps. The chemicals utilized in the pretreatment are given in Table I. Catalytic particles (Pd) replaced stannous on the fiber surface, during the process. After dried, EN film was then deposited from electrolytic solutions. The composition

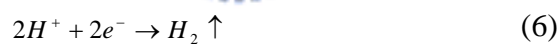
and operating condition of EN plating bath are listed in Table II. The surface of the EN films was examined by using Field Emission Scanning Electron Microscopy (FESEM).

Electroless deposition is a chemical reaction process. From the proposed reaction mechanisms, it is generally accepted that the overall reaction in electroless plating of two kinds of simultaneous reactions [19]:

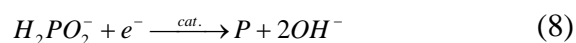
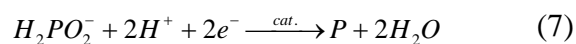
(i). Anodic reaction:



(ii). Cathodic reaction:



The codeposition of phosphorus in most electroless solutions with hypophosphite as the reductant is a third cathodic reaction.



These chemical reactions explain the anodic oxidation of the reducing agent and the cathodic production of metal and hydrogen.

. Results and Discussion

Figure 4-3 illustrates a fiber spreading experiment, while the $V_F = 7$ m/min and $Q < 60$ L/min, where V_F is the fiber transporting velocity and Q is the flux. The fiber tow was difficult to be spread by air drag owing to the small air velocity; therefore, it kept the original size about 5 mm as shown in Fig. 4-3(a). The fibers were spread in width about 20 mm at fiber exit under $V_F = 7$ m/min and $Q = 70$ L/min as shown in Fig. 4-3(b). It has been investigated that the velocity of airflow had extremely small difference between inlet-1 and inlet-2 by our previous study [17]. It is well known that $Q = \rho UA$, where Q is the flux; ρ is the fluid density; U is the fluid velocity, and A is the cross-section area of inlet. When air was sucked into the spreader, varieties of air velocity appeared at inlet-1, inlet-2 and slots, since the cross-section area decreased. Furthermore, the flux at inlet-1 was 10 times larger than that at inlet-2, and the slots on the clapboard were close to the inlet-1; hence, the main variations in air velocity would occur at inlet-1 nearby. The fiber tow was transported into the spreader and the fiber tow was spread out and fluffed at the fiber exit (i.e. inlet-1). This is because that the airflow was accelerated and a maximum axial velocity of airflow was produced at the fiber exit when air was sucked into the spreader. While the flux Q was increased upto 90 L/min, it was seen that the fiber tow was easily spread, and the most fibers were dragged toward the clapboard and concentrated at the clapboard side. As shown in Fig. 4-3(c), the carbon fiber tow was spread at 50 mm in width. During the spreading process, the spread fibers were gradually extended to the clapboard by the large axial velocity. The distribution of the lateral velocity increased abruptly near the clapboard, since the airflow turned toward the slots in the spreader. Thus, as air flowed into the inner location, axial velocity decreased [17]. The air cross-flow provided a drag force on the carbon fibers. Finally, the fibers were dragged toward the

clapboards and kept the same width as the fiber exit. Similar spread results were obtained for other conditions with the same spreading procedures. The continuous fiber spreading procedures can be summarized into three main steps recounted as follows:

- (1) The fiber tow was firstly spread out and fluffed at the fiber exit by the axial airflow.
- (2) Fibers gradually moved toward lateral side, and the lateral velocity would influence the fiber movement.
- (3) As the fibers moved closer to the clapboard, the transverse velocity increased; hence, the fibers were dragged toward the clapboard.

The proposed spreading procedures were more detailed and quite different from the procedures proposed by previous investigators. Fig. 4-4 indicates the width of the unspread and spread fiber tow under different test conditions. To study the spreading evenness of the carbon fiber tow by the pneumatic spreading system, the area fraction of the fiber tow in 50×50 (mm²) area was calculated by the above mentioned method and the evenness of the spread fiber tow was thus obtained. The spreading evenness in Fig. 4-4(a) ~ 4-4(c) was 10 (%), 36.3 (%) and 37.8 (%), respectively. The difference of the evenness can be realized by previous discussion. The spreading evenness was increased with air flux at the same fiber transporting velocity, but it was decreased as the air flux increased beyond 80 L/min owing to the lateral velocity too large. We can obtain good spreading evenness under a certain condition and it can be seen from Fig. 4-5. Similar trends were observed at others fiber transporting velocity. It was also found that the evenness was better at low fiber transporting velocity than that at high fiber transporting velocity for a small air flux, such as $Q = 70$ L/min. However, more the transporting velocity increased, more the evenness improved at a large air flux,

such as $Q = 80$ L/min. This is because the axial velocity is dominated at the fiber exit for a small air flux. There was a long interaction time between airflow and fibers at a low fiber transporting velocity. Therefore, the fibers were spread out and fluffed obviously. Similarly, the lateral velocity is dominated near the clapboard for a large air flux; a low transporting velocity resulted in a long interaction time between airflow and fibers; hence, more fibers were dragged to the clapboard. A little difference was observed on the evenness at $Q = 90$ L/min for the three fiber transporting velocity due to the lateral velocity dominated. From the spreading evenness, the quantitative comparison was easily made with the different spread fiber tow under the different test conditions.

Figure 4-6 presents that the spread fiber tow under $V_F = 7$ m/min and $Q = 80$ L/min has the spread evenness of 61.3(%). However, the result was not satisfied, because the evenness of a spread carbon fiber tow was restrained from large lateral air velocity. For this reason, we sealed 8 slots in the spreader; only the first slot opened. Therefore, when the air flux was increased, the air was quickly sucked into the spreader and the airflow passed through the first slot to the outlet. The main air velocity was the axial velocity and the coverage of lateral air velocity was reduced with decreasing the slots on the clapboard. Hence, the fiber tow was transported into the spreader and fibers were separated and moved to the lateral side by the axial velocity. Fiber tow would not be influenced by large drag force due to a small lateral velocity. As a result, the spreading evenness was promoted in a carbon fiber tow, and fibers spread out smoothly. The calculated spreading evenness could get up to 72 (%) under $V_F = 7$ m/min and $Q = 105$ L/min.

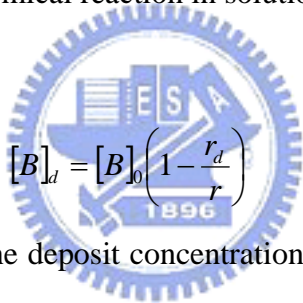
To investigate the improvement of fiber coating by fiber pneumatic spreading process, both spread (evenness = 72%) and original unspread carbon fiber tow were

dealt with the two-step pretreatment to initiate the EN deposition as shown in Fig. 4-7(a). The two activated fiber tows were simultaneously placed in identical electrolytical conditions for 15 min. Fig. 4-8(a) exhibits a surface morphology of the original fibers. It seems to be a bark-like contour; details of the image are shown in Fig. 4-9(a). The uneven surface will enhance mechanical interlock between the fiber and Ni deposit. Fig. 4-8(b), and 4-8(c) are the samples taken from inner and outer part of the unspread carbon fiber tow as shown in Fig. 4-7(b), location A and D, respectively. They show a clear distinction in Ni films. The fibers at the outer part were completely covered by Ni coating, but fibers at the inner part were partially coated. This is caused by a different deposition rate and there is a slow growth rate in inner part as shown in Fig. 4-8(c).

Microstructure observed in the case of Fig. 4-8(b) and 4-8(c) was presented in Fig. 4-9(b) and 4-9(c), respectively. A different growth mode was obvious between the outer part and inner part of the unspread fiber tow. It is interesting to note that the nickel grains are not single crystals but consist of massive aggregates of smaller crystallites of size about 20~30 nm in diameter as shown in Fig. 4-9(b). These results suggested that the electroless deposition is mainly the result of the continuous nucleation of crystallite and their three-dimensional growth, due to a fast chemical reaction. The results are consistent with *in situ* STM observation [20]. However, a particle size about 200 nm was also observed as shown in Fig. 4-9(c) and it is mainly a crystal growth due to a slow chemical reaction. The observation is consistent with Sard investigated in electroless copper deposits [21]. He argued that the copper crystals obtained under a more dilute solution have several thousand angstroms in size and differ from the one in that there are many aggregates of crystallites. This is a reason why previous investigators argued that the Ni coating may not be possible to

coat less than 0.2 μm . But these differences had never been proposed by previous investigators. Moreover, these results implied a concentration gradient existed in the chemical reaction and a different reaction mechanism controlled the EN deposition. For the spread carbon fiber tow, a similar surface morphology was observed as shown in Fig. 4-8(b), and a homogeneous reaction was obtained.

The observed variations on the Ni coating were very obvious; therefore, the Ni thickness at various depths in a carbon fiber tow was estimated by typical transverse cross-section. The fibers were taken from unspread fiber tow at depth A, B, C, and D respectively, as shown in Fig. 4-7(b). To compare with the electroless plating reaction between the unspread and spread carbon fiber tows, we followed Eqn. (1) of reaction kinetics, which describes a chemical reaction in solution [22].



$$[B]_d = [B]_0 \left(1 - \frac{r_d}{r} \right) \quad (1)$$

Here, both $[B]_d$ and $[B]_0$ are the deposit concentration at a given distance and outside of the fiber tow, respectively. The r_d is the given distance from center to a given point, and r is the distance from the center to the periphery, which is 1.75mm and $d/2$ for the unspread and spread carbon fiber tow, respectively. Eqn. (1) can be rewritten as follows:

$$\frac{r_d}{r} = \left(1 - \frac{[B]_d}{[B]_0} \right) \quad (1)'$$

Hence, a normalized depth (r_d/r) from center to the outside of a fiber tow versus Ni thickness $[B]_d$ was obtained as illustrated in Fig. 4-10. The results represent that Ni thickness was decreased along the distance for the unspread carbon fiber tow at

deposition time of 15 and 5 min. From the reaction kinetics, this deposit concentration dependent distance is a diffusion-controlled reaction. It was fairly realized that the reactants did not easily diffuse into the inner fibers due to the closely compact fibers in a tow. This phenomenon can be confirmed by Fig. 4-8. On the contrary, there was a uniform nickel thickness in the spread carbon fiber tow. This is because there was no diffusion in the reaction process; therefore, the reactant concentration stayed constant at the fiber surrounding. Consequently, the chemical reaction process was governed by the surface reaction-controlled or activation-controlled reaction. For the electroless plating deposition is a rate-determining step reaction, once the concentration gradient occurs in solution, diffusion is dominant in the reaction.

Two intersections can be seen in Fig. 4-10. The intersection for the deposition time of 15 min intercepted the normalized distance at 0.92, i.e. $r_d=1.61$ mm. For fibers located between center and 1.61 mm in the unspread carbon fiber tow, the electroless plating reaction is a diffusion-controlled reaction. By contrast, for fibers located between 1.61 mm and the periphery of the fiber tow, the electroless process is an activation-controlled reaction. It is important to note that two different reaction mechanisms simultaneously occur in the unspread carbon tow, as the electroless plating reaction proceed. As a result, the thickness of fiber layers that underwent activation-controlled reaction was 0.14 mm, which corresponds to 20 fiber layers. The layers are still larger than the maximum distribution of about 10 layers in the spread carbon fiber tow. Similar results can be obtained from another intersection, but the range occurred diffusion-controlled reaction was slightly narrowed. The reason is the concentration of the reactants decreases with increasing deposition time; thus, the concentration gradient arises more easily as a result of a difficult diffusion. As more fibers are uniformly spread out, coating thickness is more even on each fiber due to no

concentration gradient.

Codeposition of phosphorus would be taken place during the electroless process. The phosphorus contents in Ni coating were examined by Inductively Coupled Plasma-Mass (ICP-Mass) as shown in Fig. 4-11. The fibers were taken from location A and D in the unspread fiber tow, as shown in Fig. 4-7(b). For the spread fiber tow, the fibers were taken center and the side as shown in Fig. 4-7(b). The results indicated that the inner fibers taken from location A have lower phosphorus contents in the unspread fiber tow, but the rest have similar phosphorus contents. As mentioned above, The electroless process is the result of the anodic oxidation of the hypophosphite and the Ni ion reduction in cathode. Reaction (1) is the dehydrogenation of the hypophosphite at the activated surface. While reaction (2) and (3) are accelerated, cathodic reaction would be promoted. Because pH is quickly dropped with the $[H^+]$ produced and $[OH^-]$ consumed in the EN solution, phosphorus accompanying Ni is deposited by reaction (7). It is very clear why the rest of the samples have higher phosphorus contents.

However, to explain the lower phosphorus contents at location A, we have to account for reaction (3), (4), (5) and (6). By reaction (3) and (4), the free radical HPO_2^- oxidized in solution and hydrogen atoms recombined with each other. Without continuous supply of hypophosphite by bulk solution, the hypophosphite would be quickly depleted in the inside of the unspread tow; hence, the concentration gradient arose. Furthermore, reaction (5) and (6) competed with each other at the fiber surface and the competition greatly decreased the reducing efficiency of the hypophosphite. Thus, a little Ni was deposited and the codeposition of phosphorus was restrained in the inner fibers of the unspread fiber tow, so the nucleation rate was slower than growth rate. It can be confirmed that there exist two different growth modes in a

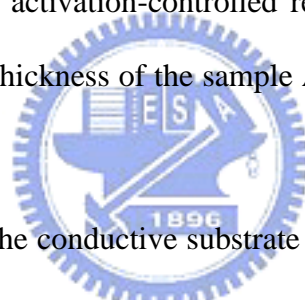
carbon fiber tow as illustrated in Fig. 4-7.

Figure 4-12(a) and 4-12(b) were the energy dispersive spectroscopy (EDS) analysis of Fig. 4-8(b) and 4-8(c), respectively. The investigation has revealed that phosphorus was observed at outer fibers as illustrated in Fig. 4-12(a), but only nickel was measured at inner fibers as shown in Fig. 4-12(b). The result obtained from inner fibers was disagreed with Svendsen proposed [23]. He suggested that the increase in phosphorus content for the very thin layer deposited in the initial plating stage was caused by the presence of decomposition reaction of hypophosphite due to the direct contact of Pd catalyst, such as reaction (8). However, if the reductant of hypophosphite is diluted in the EN solution. The Ni would be deposited only under our operating conditions. Meanwhile, Au sputtered on the fiber surface was detected to avoid charge by primary electron.

Touhami has suggested that hypophosphite concentration has a marked effect in the reduction process, but the concentration of Ni ion is not very pronounced [24]. It can be asserted that the diffusion-controlled reaction is caused by hypophosphite lacked in the inside of the unspread carbon fiber tow. In addition, it can be observed that there are higher phosphorus contents at the first 5 min than that at other deposition time. This consequence agreed with that the phosphorus contents are higher at initial stage in EN deposition by previous works [25]. The Pd surface has a high specific activity for the oxidation process at redox reaction. Thus, the rate of the hypophosphite oxidation reaction is very high. At the Pd/solution interface, the pH of the solution is reduced due to reaction (7). At the same time, the rate of the reaction of phosphorus deposition is increased. Because of this condition at the interface, the initial stage of deposition will give a nickel deposit with higher phosphorus contents.

To evaluate the catalytic effect for an unspread carbon fiber tow, after Pd activation,

we extracted fibers from location A as shown in Fig. 4-7(b). Both sample A and spread fibers were placed in an EN bath for 10 min. The surface and fracture morphology of the samples was presented in Fig. 4-13 and 4-14. It can be seen in Fig. 4-13(a) and 4-13(b) that both sample A and spread fibers have similar surface morphology and 3-D nucleation growth mode. In addition, the difference in thickness was about 60-80 nm as shown in Fig. 4-14(a) and 4-14(b). Similarly, the grain was the aggregates of much finer crystallites about 30 nm in size. The results indicate that both the sensitization and activation steps have no significant effect to the electroless reaction process under our operating conditions. Particularly, morphology observed on sample A was very different from that the morphology in Fig. 4-8(c). The main factor is that the overall reaction is activation-controlled reaction because of no diffusion occurred; in spite that the Ni thickness of the sample A is slightly less than that of the spread fibers.



Nucleation and growth on the conductive substrate are in a high reaction rate at the initial stage; the electroless reaction is based on the electrochemical mechanism [19]. The phenomena can be confirmed by Fig. 4-15(a). The image showed high dense nuclei on the spread fibers as a spread carbon fiber tow placed in an EN bath for 3 min. It was in good agreement with previous investigation. Hence, the result strongly indicates that the mechanism is an electrochemical one. After the spread carbon fiber tow were placed in an EN bath for 5 min, a thin and uniform nickel film was obtained on each fiber. The thickness of the Ni film was only about 0.1 μm as illustrated in Fig. 4-15(b), and it is important to note that carbon fiber can easily be coated less than 0.2 μm by the pneumatic spreading system, even though the carbon fiber tow contains 12k fibers. Langdry has argued that the coating on the fibers on the outside of the tow would be extremely thick, while the fibers at the center of the tow would remain

uncoated due to shadowing, if reactants decomposition was taking place exclusively [15]. From our results, a restricted conclusion will be that the shadowing is caused by the compact fibers in a tow; therefore, the reactants could not penetrate into the inner part of a tow. However, by the fiber pneumatic spreading system, a carbon fiber tow can be smoothly spread out; then a metallic or non-metallic film can be uniformly coated on each fiber in the spread fiber tow.



.Conclusion

In this study, by the fiber pneumatic spreading system, a thin and uniform nickel film was successfully coated in a carbon fiber tow. The carbon fiber tow was easily spread out at the test conditions and the performance was better than the previous studies. Additionally, the evaluation of the spreading evenness was constructed, and the quantitative comparison can be achieved in the spreading process. The major results and conclusions from this work are summarized as follows:

- (1). The spreading evenness, a new variable, was constructed. The quantitative comparison is easily made with the different spread fiber under the different test conditions, and the optimum condition in spreading process can be obtained by the spreading evenness.
- (2). The spreading evenness for a carbon fiber tow was restrained from large lateral air velocity; therefore, the coverage of the lateral air velocity can be reduced when 8 slots were sealed in the spreader. The spreading evenness of the carbon fiber tow can get up to 72 (%).
- (3). The spreading evenness is first used and discussed in spread carbon fiber tow, and it is more useful than spreading degree for the spreading process of the fiber tow.
- (4). Two different controlled reaction mechanism simultaneously occur in a unspread carbon fiber tow as the electroless plating reaction proceeding, which resulted in non-uniform nickel coating, one is diffusion-controlled reaction; another is activation-controlled reaction. For the spread fiber tow, the chemical reaction process is governed by the activation-controlled reaction.
- (5). For the unspread fiber tow, the main factor of the diffusion-controlled reaction is concentration gradient, which is caused by hypophosphite depleted in the inside

of a carbon fiber tow.

- (6). This is the first time that the thickness of the Ni coating can be coated on carbon fiber tow less than $0.2 \mu\text{m}$.
- (7). By the fiber pneumatic spreading system, a carbon fiber tow can be uniformly spread out, and an uniform Ni coating can be obtained on each fiber. The system can be applied to get a thin and uniform metallic or non-metallic film for a fiber tow.



. References

- [1] Chi-Yuan Hung and Jui-Fen Pai: Eur. Polym. J., 1998, vol. 34, No. 2, pp. 261 – 267.
- [2] Guanghong Lu, Xiaotian Li and Hancheng Jiang: Composites Science and Technology, 1996, vol. 56, pp. 193 - 200.
- [3] B. Wielage and A. Dorner: Composites Science and Technology, 1999, vol. 59, pp. 1239 - 1245.
- [4] Ziyuan Shi, Xuezhi Wang and Zhimin Ding: Applied Surface Science, 1999, vol. 140, pp. 106 – 110.
- [5] J.K. Yu, H.L. Li, and B.L. Shang: Journal of Material Science, 1994, vol. 29, pp. 2641 - 2647.
- [6] Susan Abraham, B.C. Pai, K. G. Satyanarayana, and V. K. Vaidyan: Journal of Materials Science, 1990, vol. 25, pp. 2839 -2845.
- [7] S. Abraham, B.C. Pai, and K. G. Satyanaryana: Journal of Materials Science, 1992, vol. 27, pp. 3479 - 3486.
- [8] H. M. Cheng, A. Kitahara, S. Akiyama, K. Kobayashi, and B. L. Zhou: Journal of Materials Science, 1992, vol. 27, pp. 3617 - 3623.
- [9] Wang Yu-Qing, and Zhou Ben-Liam: Journal of Materials Processing Technology, 1998, vol. 73, pp. 78 - 81.
- [10] R.J. Bobka and L. P. Lowell: Handbook of Composites, vol. 1- Strong Fibers, W. Watt, and B.V. Perov, eds., Elsevier Science Publisher B.V., 1985, pp. 579-80.
- [11] Clark, D., N.J. Wadsworth, and W. Watt: Handbook of Composites, vol. 1- Strong Fibers, W. Watt, and B.V. Perov, eds., Elsevier Science Publisher B.V., 1985, pp. 579-80.

- [12] G. Leonhardt, E. Kieselstein, H. Podlesak, E. Than, and A. Hofman: *Materials Science and Engineering*, 1991, A135, pp. 157 - 160.
- [13] J.K. Yu, H.L. Li, and B.L. Shang: *Journal of Material Science*, 1994, vol. 29, pp. 2641 - 2647.
- [14] R. V. Subramanian and A. Nyberg: *J. Mater. Res.*, 1992, vol. 7, pp. 677 - 688.
- [15] Christopher C. Langdry and Andrew R. Barron: *Carbon*, 1995, vol. 33, No.4, pp. 381 - 387.
- [16] Shojiro Ochiai and Yotaro Murakami: *Journal of Materials Science*, 1979, vol. 14, pp. 831 - 840.
- [17] J. C. Chen and C.G Chao: *Metallurgical and Materials Transactions B*, 2001, vol. 32B, pp. 329 - 341.
- [18] J. P. Marton and M. Schlesinger: *J. Electrochem. Soc.*, 1968, vol. 115, pp. 16 – 21.
- [19] Bing Joe Hwang and Sheng Horng Lin: *J. Electrochem. Soc.*, 1995, vol. 142, No.11, pp. 3749 - 3754.
- [20] Takayuki Homma, Takuya Yamazaki, and Tetsuya Osaka: *J. Electrochem. Soc.*, 1992, vol. 139, No. 3, pp. 732 - 736.
- [21] Richard Sard: *J. Electrochem. Soc.*, 1970, vol. 117, No. 7, pp. 864 - 870.
- [22] Michael J. Pilling and Paul W. Seakins: *Reaction Kinetics*, Oxford University Press, 1995, pp. 143 - 158.
- [23] Leo G. Svendsen: *J. Electrochem. Soc.*, 1983, vol. 130, No.11, pp. 2252 – 2255.
- [24] Valery M. Dubin: *J. Electrochem. Soc.*, 1992, vol. 139, No. 5, pp. 1289 - 1294.
- [25] M. Ebn Touhami, M. Cherkaoui, A. Srhiri, and A. Ben Bachir: *Journal of Applied Electrochemistry*, 1996, vol. 26, PP. 487 - 491.

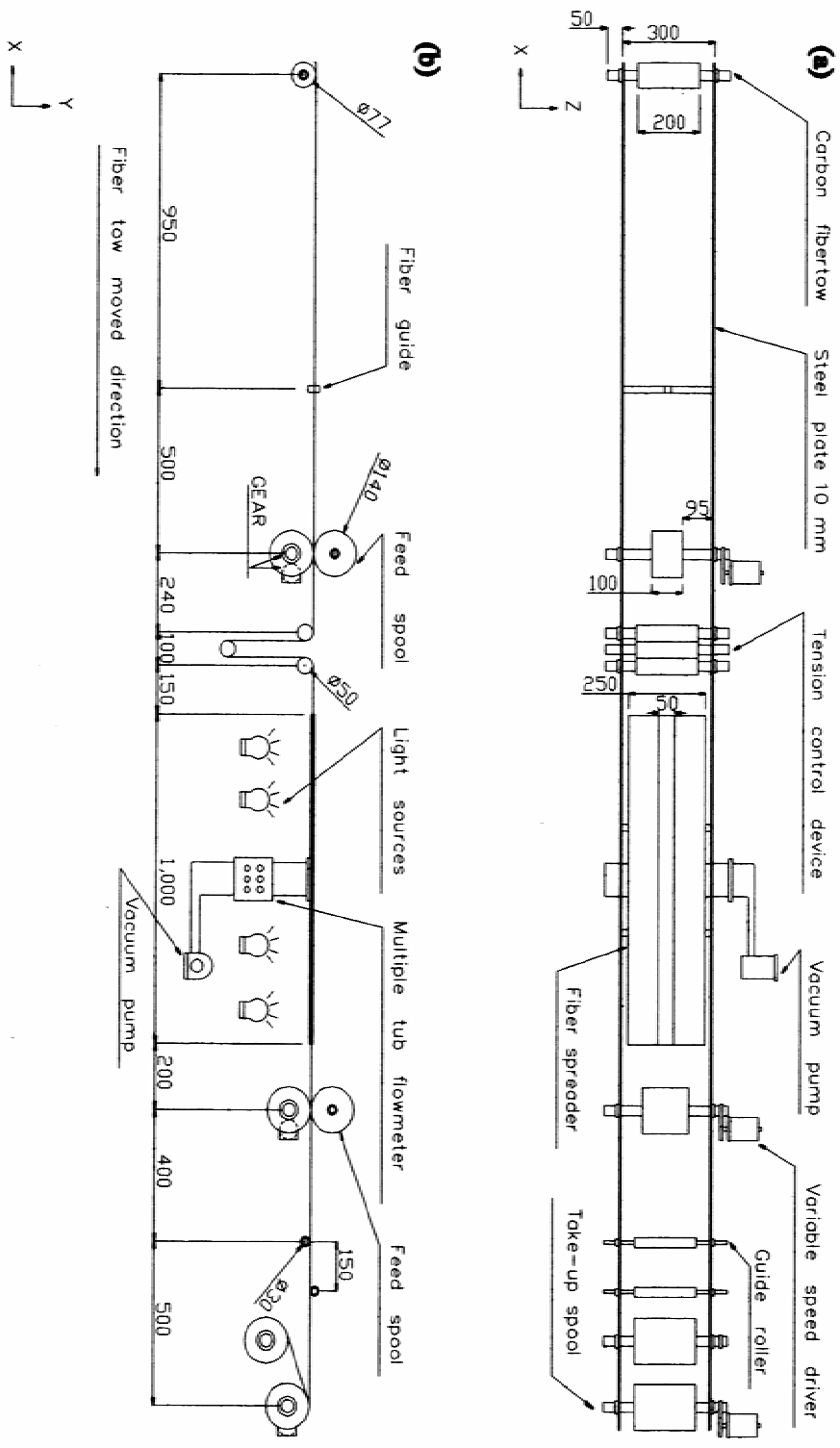


Fig. 4-1 Schematic of the experimental setup for spreading carbon fiber tow (a) top view and (b) side view.

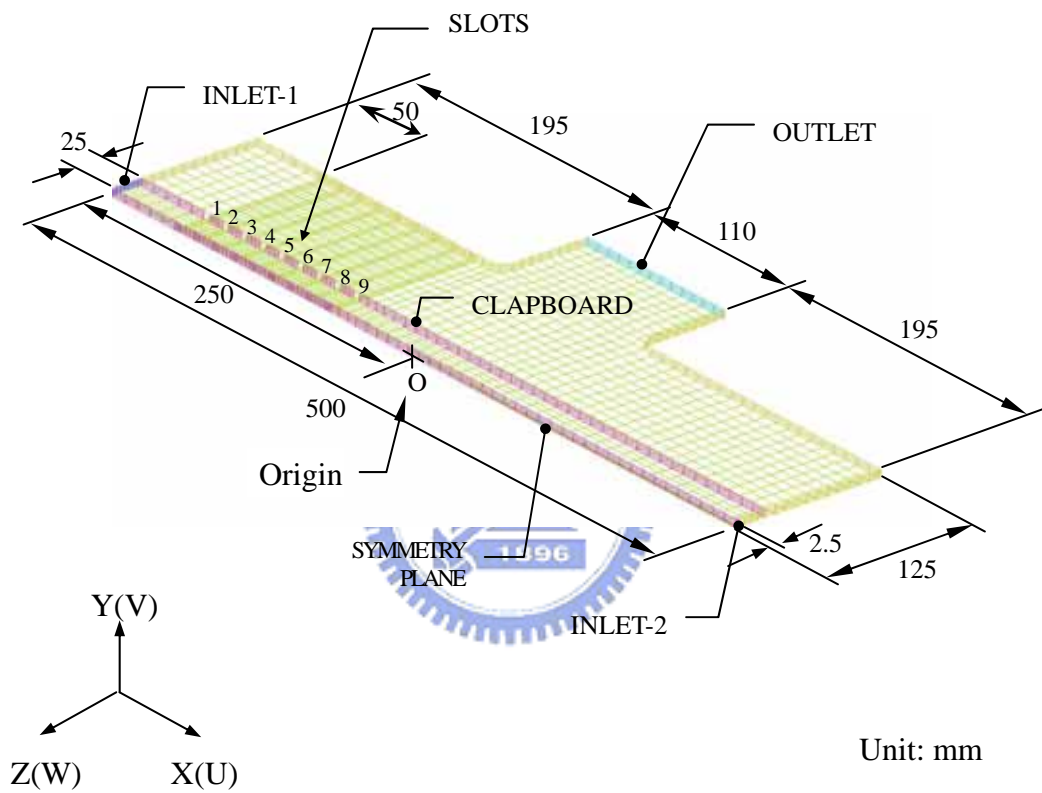


Fig. 4-2 A perspective of the pneumatic spreader in a isometric view.

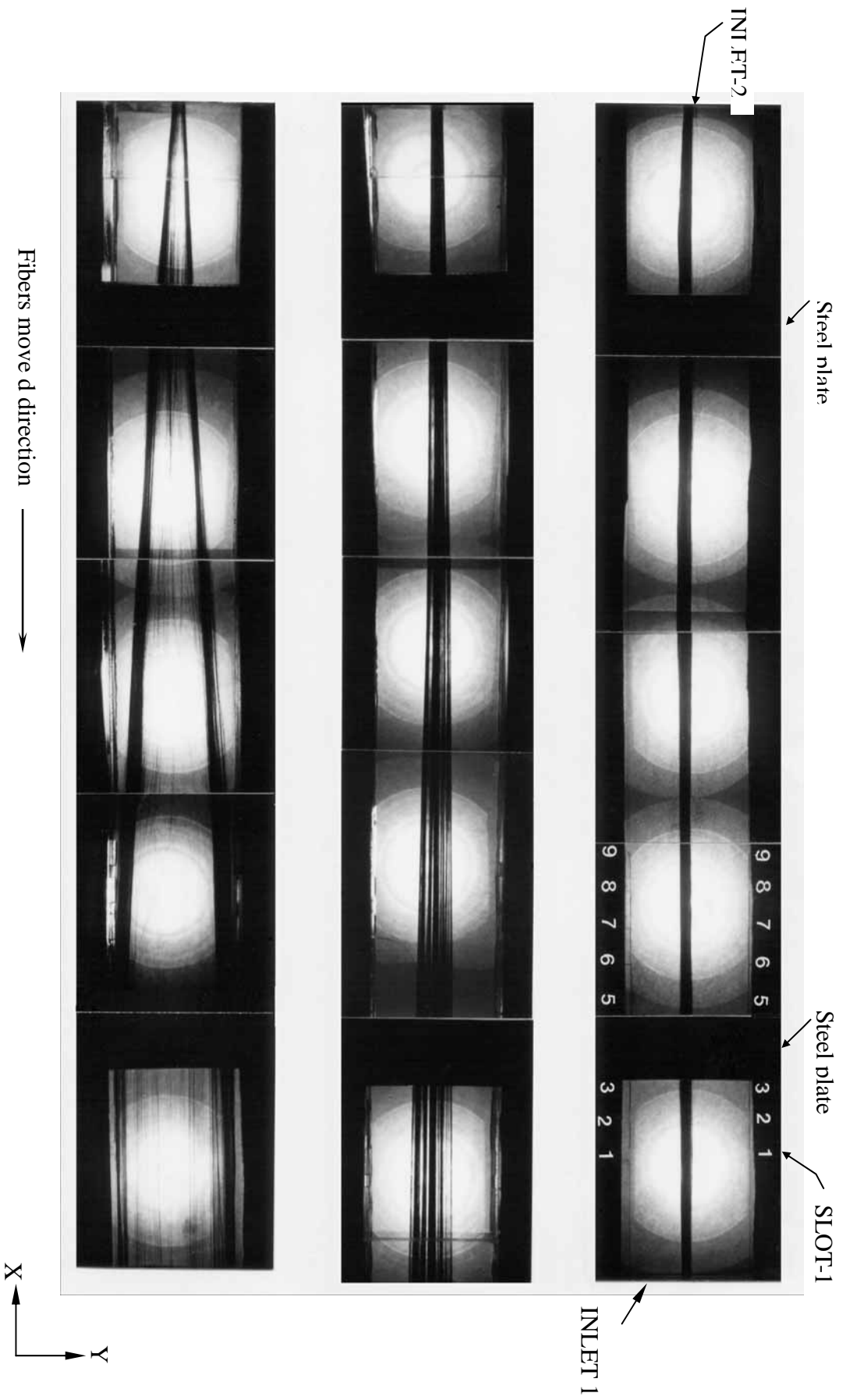
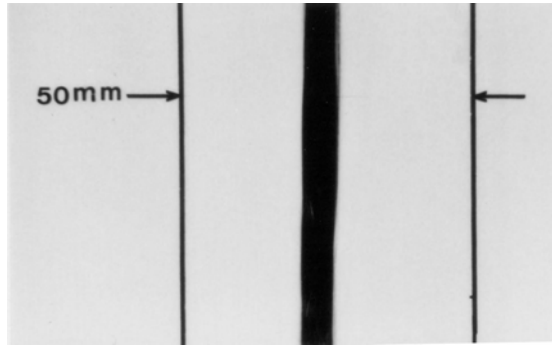
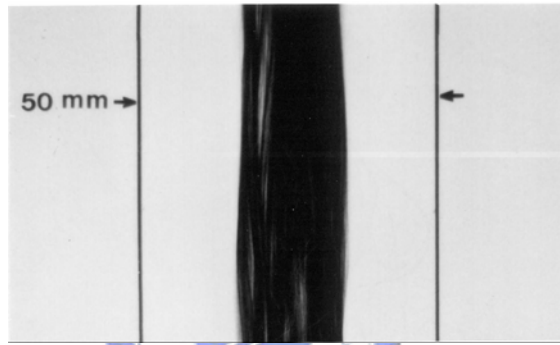


Fig. 4-3. Photographs of carbon fibers spread experiment under (a) $V_F = 7$ m/min and $Q < 60$ L/min, (b) $V_F = 7$ m/min and $Q = 70$ L/min and (c) $V_F = 7$ m/min and $Q = 90$ L/min.



(a)



(b)



(c)

Fig. 4-4 Photographs of the unsprung and spread carbon fiber tow corresponding Fig. 4-3 in different width (a) 5 mm, (b) 20 mm and (c) 50 mm.

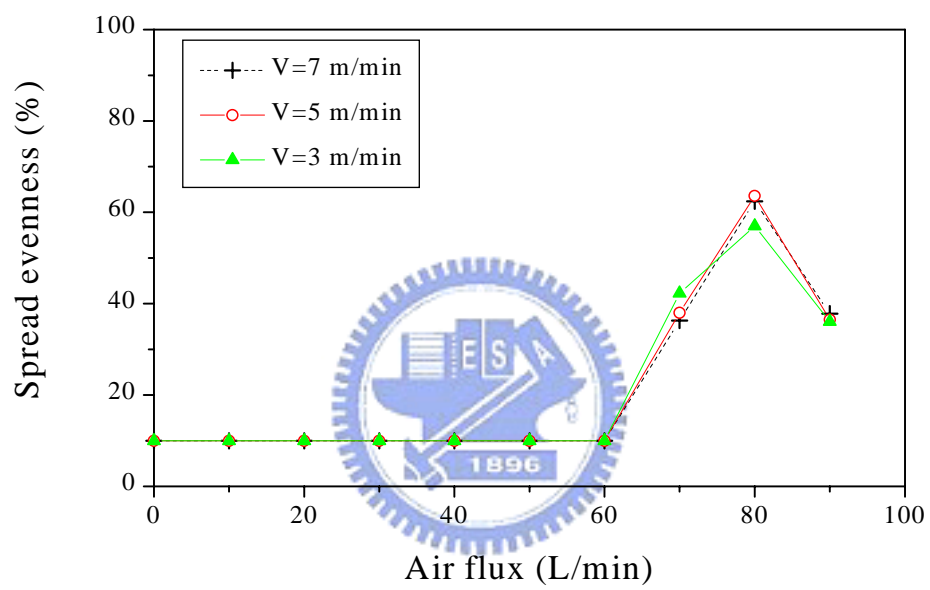


Fig. 4-5 The relations of the fiber spread evenness and the carbon fiber tow air flux under different fiber transporting velocity.

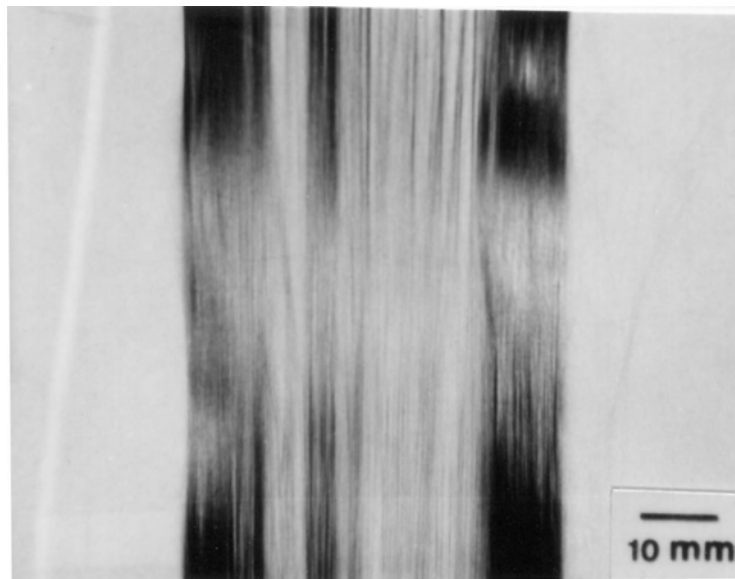


Fig. 4-6 The spreading evenness of the carbon fiber tow equivalent to 61.3 (%) under the condition $V_F = 7$ m/min and $Q = 80$ L/min

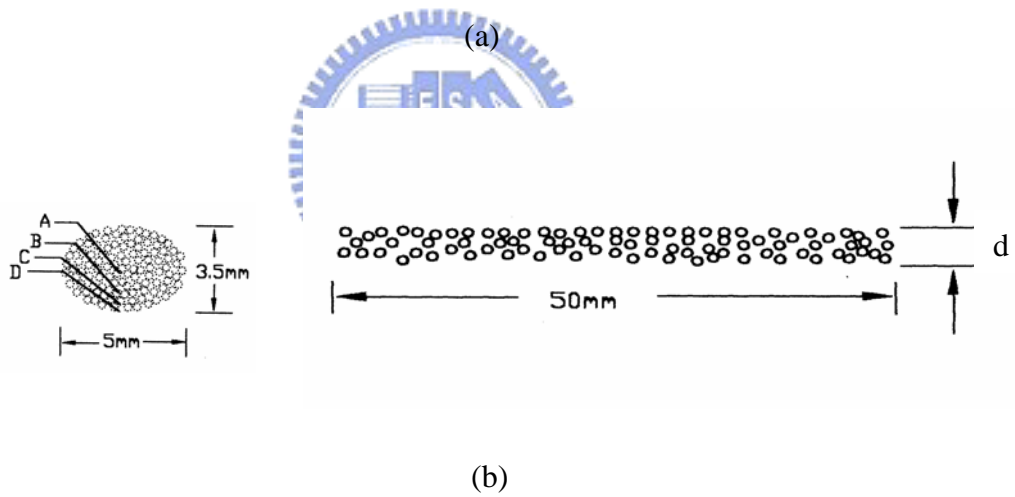
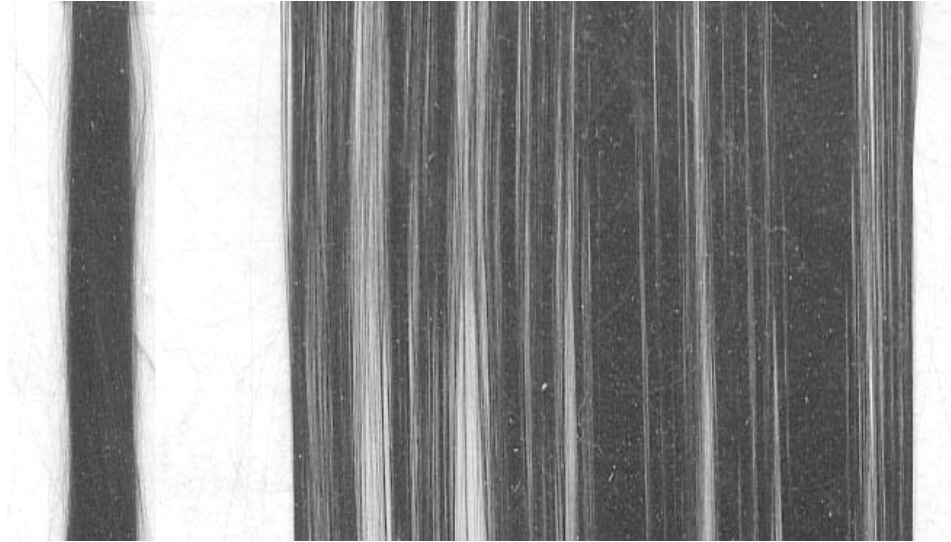
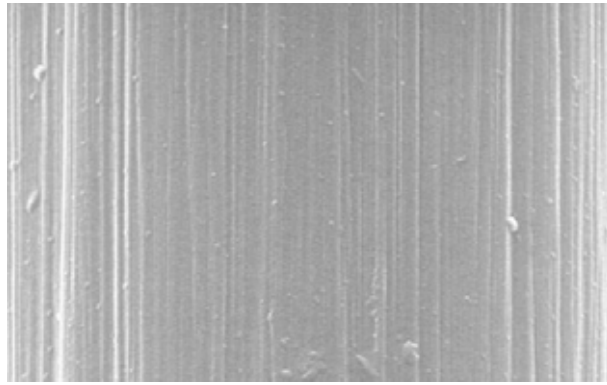
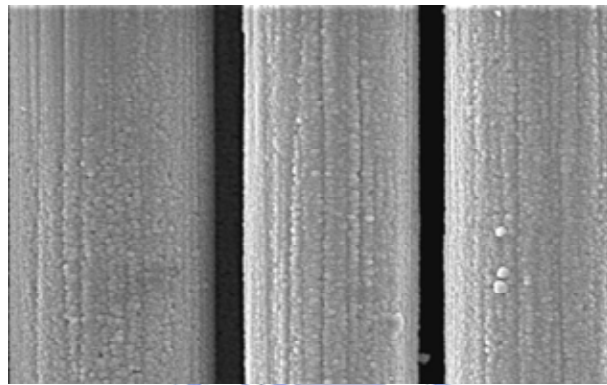


Fig. 4-7 Schematic of the unspread and spread carbon fiber tows (a) plain view (b) cross-section view, where $d=0.07$ mm.



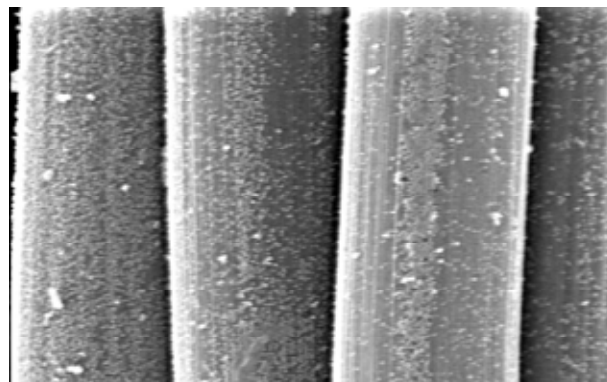
(a)

1 μm



(b)

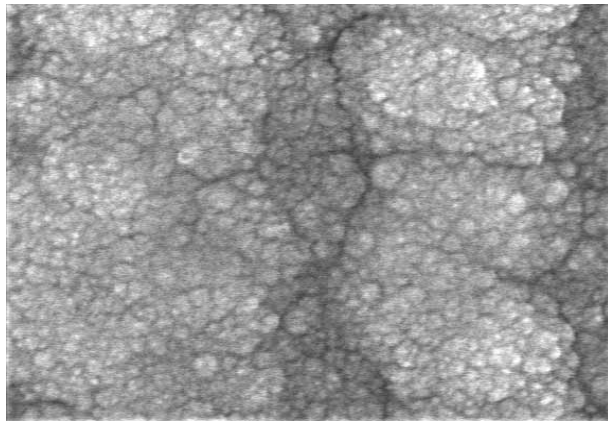
3 μm



(c)

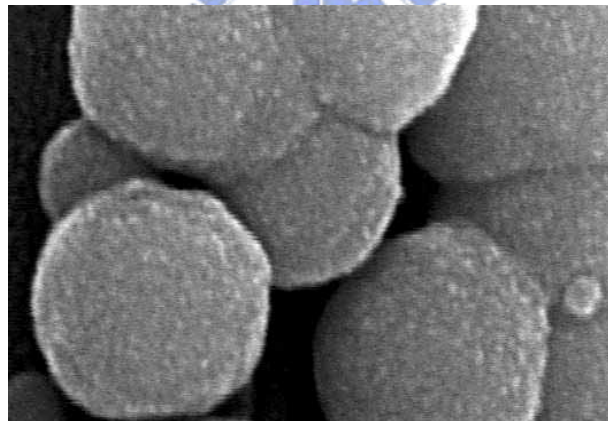
3 μm

Fig. 4-8 Surface morphology of the unspread fiber tow (a) original carbon fiber plain view, (b) and (c) as deposited outer and inner carbon fibers, by electroless nickel deposition for 15 min.



150 nm

(a)



100 nm

(b)

Fig. 4-9 Enlarged microstructure of the Fig. 4-8 (b) and (c), (a) and (b) as deposited outer and inner carbon fibers, respectively.

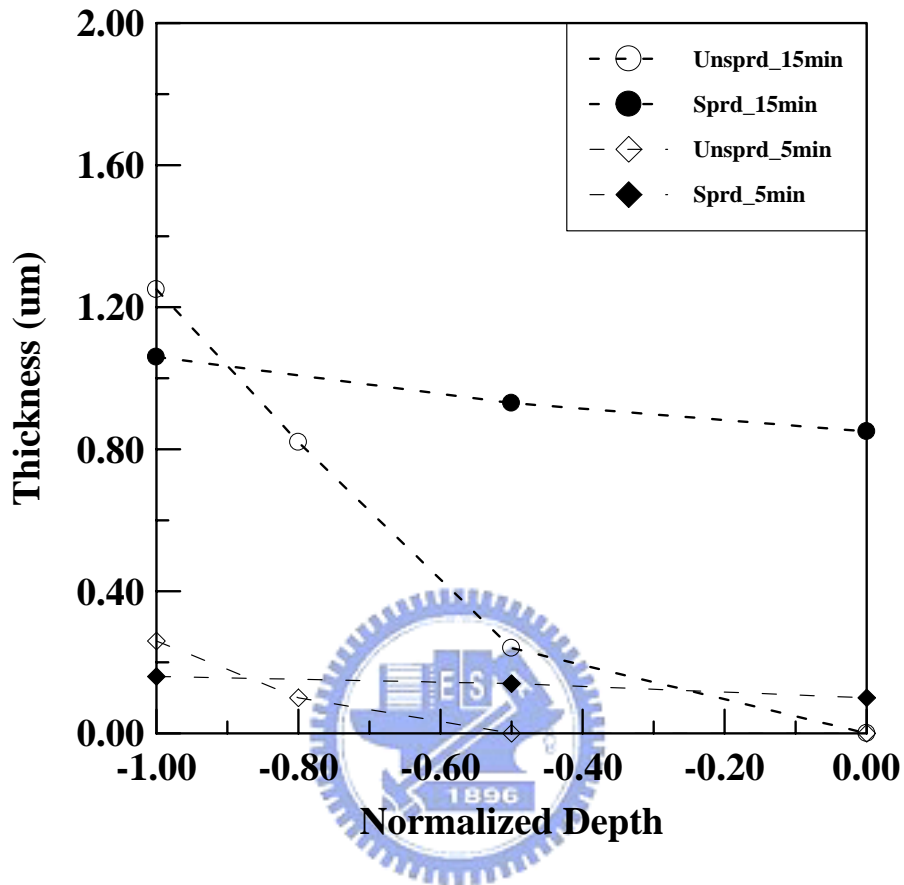


Fig. 4-10 Distribution of the nickel coating thickness at various normalized depth. (Unsprd_15min: unsprad fibers by EN de-position for 15 min, Sprd_15min: spread fibers by EN deposition for 15 min.)

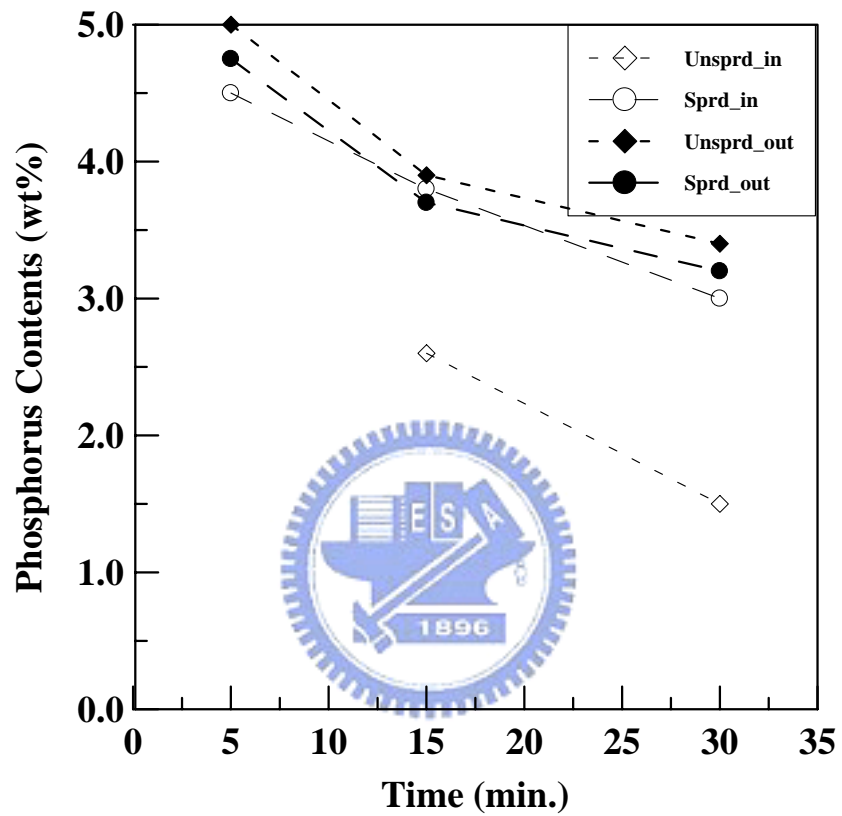
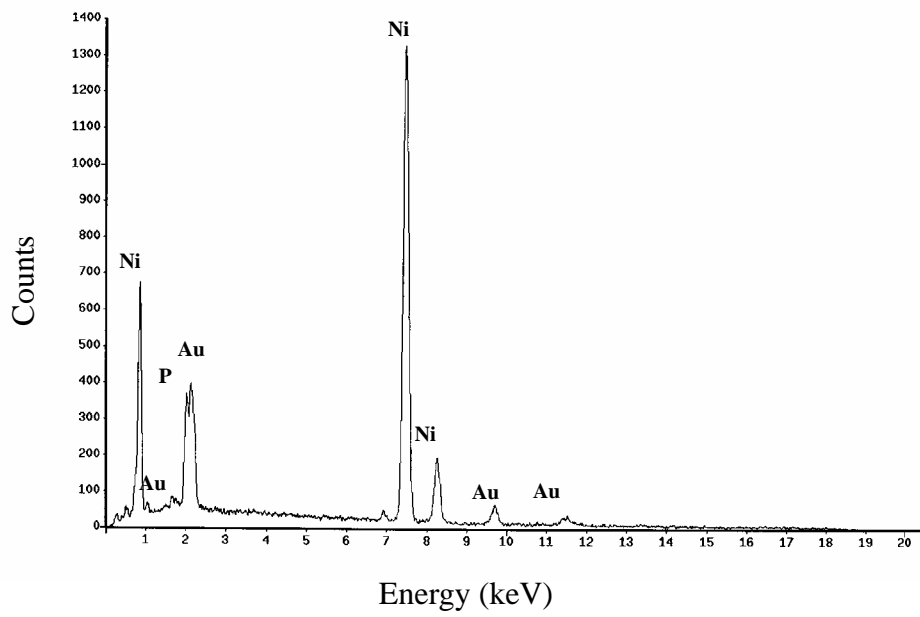
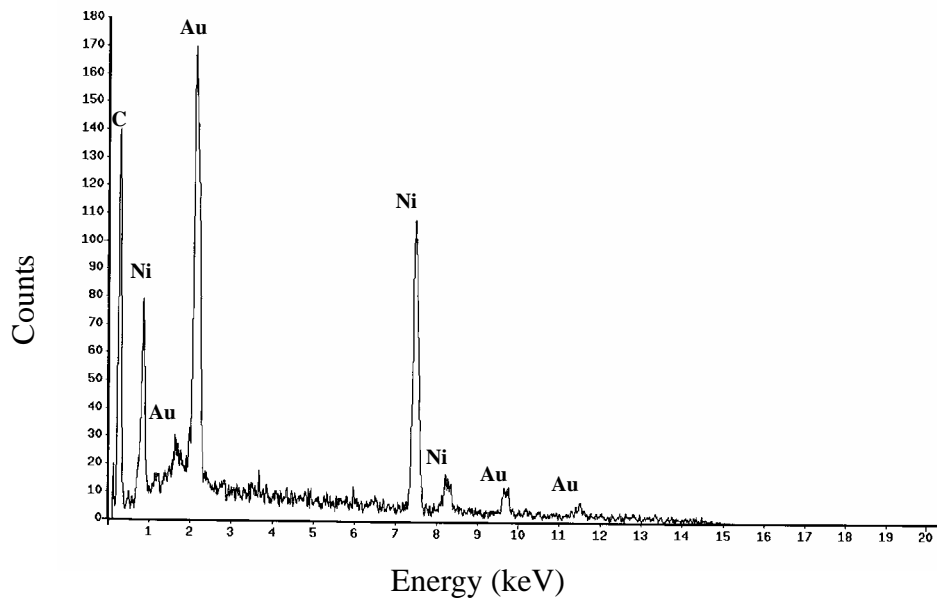


Fig. 4-11 Phosphorus contents in the nickel film at various deposition times. (Unsprd_in: inner fibers of the un_spread fiber tow, Unsprd_out: outer fibers of the unspread fiber tow, Sprd_in: inner fibers of the spread fiber tow, and Sprd_out: outer fibers of the spread fiber tow.)

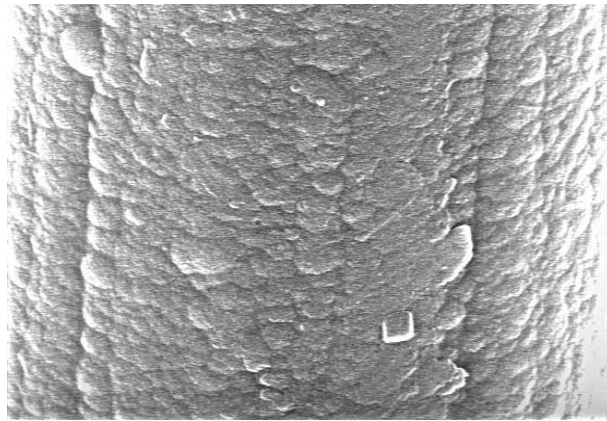


(a)

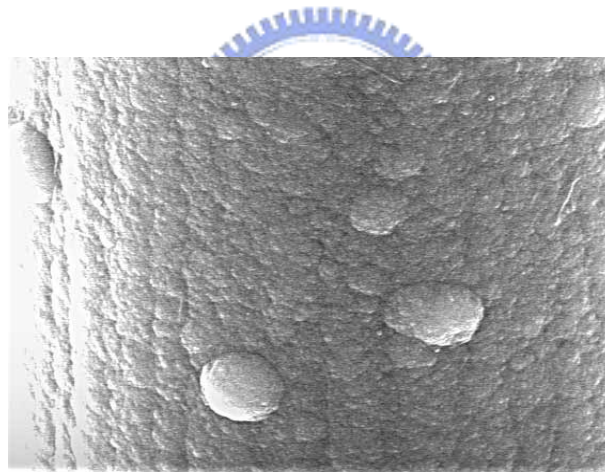


(b)

Fig. 4-12 Elements analysis for the nickel film by energy dispersive Spectroscopy (EDS) (a) the outer fibers and (b) the inner fibers of the unspread carbon

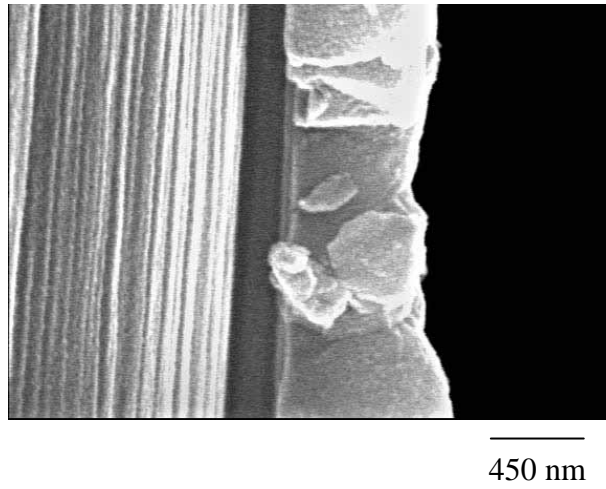


(a)

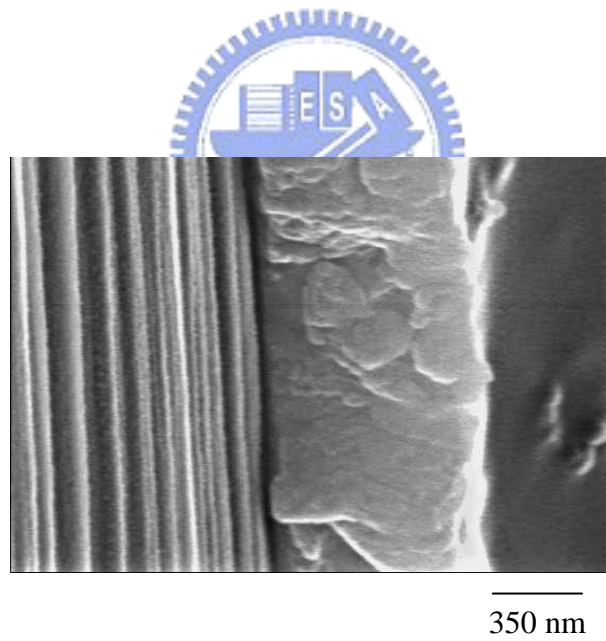


(b)

Fig. 4-13 Surface morphology of the carbon fiber tow (a) taken from an unspread carbon fiber tow at location A , and (b) taken from an unspread carbon fiber tow for the same deposition time 10 min.

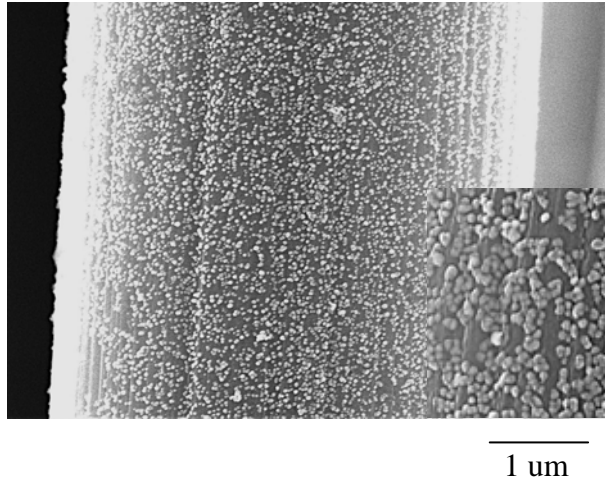


(a)

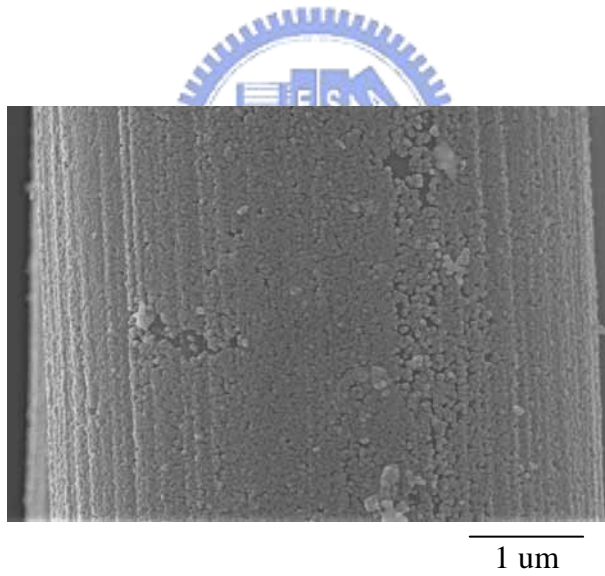


(b)

Fig. 4-14 Film thickness of as-deposited carbon fiber taken from an unspread carbon fiber tow corresponding to Fig. 4-13(a) and 4-13(b), respectively.



(a)



(b)

Fig. 4-15 Surface morphology of as-deposited carbon fiber taken from a spread carbon tow at deposition time (a) 3 min and (b) 5 min.